

GA-A24266

**ALTERNATIVE FLOWSHEETS FOR THE
SULFUR-IODINE THERMOCHEMICAL
HYDROGEN CYCLE**

by

**L.C. BROWN, R.D. LENTSCH, G.E. BESENBRUCH,
K.R. SCHULTZ, AND J.E. FUNK**

FEBRUARY 2003



GA-A24266

ALTERNATIVE FLOWSHEETS FOR THE SULFUR-IODINE THERMOCHEMICAL HYDROGEN CYCLE

by

L.C. BROWN, R.D. LENTSCH, G.E. BESENBRUCH,
K.R. SCHULTZ, AND J.E. FUNK*

This is a preprint of a paper to be presented at the 2003
Spring National Meeting of AIChE, New Orleans, Louisiana,
March 30 through April 3, 2003, and to be published in
Proceedings.

* University of Kentucky, Lexington, Kentucky.

Work supported by
the U.S. Department of Energy under
Grant No. DE-FG03-99SF21888

GENERAL ATOMICS PROJECT 30171
FEBRUARY 2003



Alternative Flowsheets for the Sulfur-Iodine Thermochemical Hydrogen Cycle

Lloyd C. Brown, Ryan D. Lentsch, Gottfried E. Besenbruch, and Kenneth R. Schultz

General Atomics

P.O. Box 85608, San Diego, California 92186-5608 USA

James E. Funk

University of Kentucky

Lexington, Kentucky 40506 USA

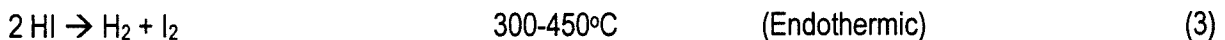
INTRODUCTION

A hydrogen economy will need significant new sources of hydrogen. Unless large-scale carbon sequestration can be economically implemented, use of hydrogen reduces greenhouse gases only if the hydrogen is produced with non-fossil energy sources. Nuclear energy is one of the limited options available. One of the promising approaches to produce large quantities of hydrogen from nuclear energy efficiently is the Sulfur-Iodine (S-I) thermochemical water-splitting cycle, driven by high temperature heat from a helium Gas-Cooled Reactor. We have completed a study of nuclear-driven thermochemical water-splitting processes. The final task of this study was the development of a flowsheet for a prototype S-I production plant. An important element of this effort was the evaluation of alternative flowsheets and selection of the reference design.

BACKGROUND

A team consisting of General Atomics, Sandia National Laboratories and the University of Kentucky recently completed a study, supported by the US Department of Energy under the Nuclear Energy Research Initiative (NERI) program, of thermochemical water-splitting processes driven by nuclear energy for the production of hydrogen [1]. In the first phase of this study [2], we reviewed the world literature on thermochemical water-splitting cycles and found 822 separate references. From these, we identified 115 different unique cycles. We evaluated these against a set of numerical criteria and identified the Sulfur-Iodine cycle as the one best suited to coupling to a nuclear reactor. In the second phase of this study [3], we reviewed the characteristics of candidate nuclear reactors for their suitability for coupling to the S-I water-splitting cycle. We identified the helium gas-cooled reactor as the one best suited for thermochemical production of hydrogen. In the third phase of this study, we completed the design of a chemical flowsheet for the S-I cycle thermochemical water-splitting process for production of hydrogen from nuclear energy [1].

The sulfur-iodine thermochemical water-splitting cycle generates hydrogen from water and thermal energy through the chemical reactions:



Sulfuric acid cannot be separated from hydrogen iodide, by thermal means, without reversing the equilibria. This separation is readily accomplished in the presence of a large excess of iodine, with the formation of two immiscible liquid phases, a light $\text{H}_2\text{SO}_4/\text{H}_2\text{O}$ phase and a heavy $\text{HI}/\text{I}_2/\text{H}_2\text{O}$ phase. Cost effective hydrogen production, using the sulfur-iodine cycle, requires that hydrogen be generated from the heavy phase efficiently and without excessive capital requirements. The Bunsen reaction, where SO_2 and I_2 are added to water to produce H_2SO_4 and HI , operates with excess water and also with excess iodine to allow separation of the H_2SO_4 and HI , and includes a boost reaction to increase the concentration of the

H_2SO_4 in water. The H_2SO_4 decomposition section includes concentration and decomposition using heat from the nuclear reactor, cascaded multiple times for efficiency, to recover the SO_2 and produce O_2 . The HI decomposition section chosen in this study uses reactive distillation of the HI , I_2 , H_2O mixture to recover I_2 and produce H_2 , but has a large recirculation flow back to the Bunsen reaction section. An overview schematic of this flowsheet is shown in Fig. 1.

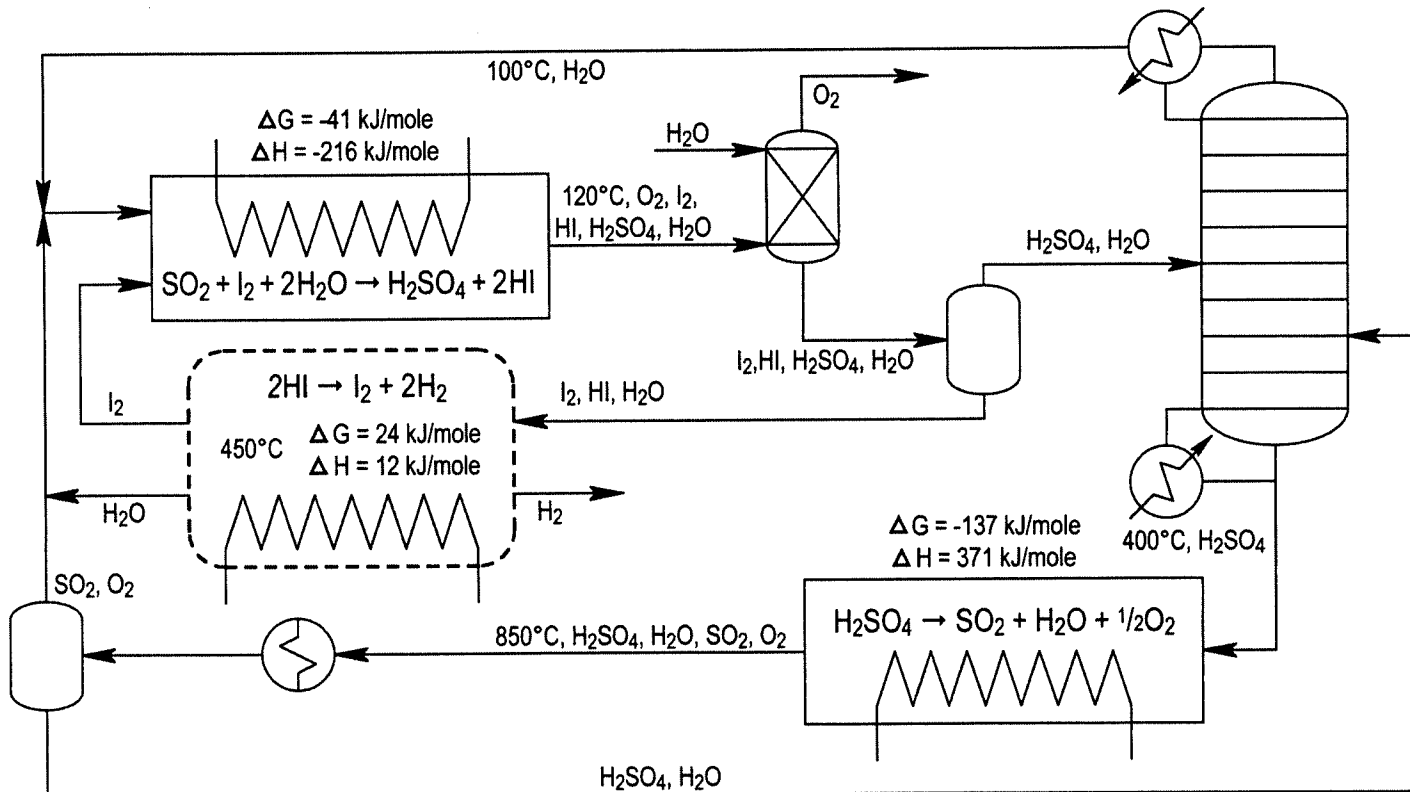


Figure 1. Overview Schematic of Sulfur-Iodine Flowsheet

FLOWSHEET DEVELOPMENT

The Sulfur-Iodine cycle consists of three coupled chemical reactions, as shown in Equations 1, 2 and 3. Sulfuric acid and hydrogen iodide are generated in the central low temperature reaction, the Bunsen reaction. Sulfuric acid is decomposed at high temperature and hydrogen iodide at lower temperatures. There are significant chemical separations associated with each chemical reaction. Water is the primary solvent in the system and iodine is also an important solvent in the Bunsen reaction.

The Sulfur-Iodine cycle was studied extensively in the 1970's and 80's. Two flowsheets were developed, the 1979 flowsheet [4], which matched the cycle to an advanced High Temperature Gas-cooled Reactor (HTGR) and a 1981 flowsheet [4,5] that was open ended, permitting the cycle to be matched to a number of thermal sources. Each flowsheet was separated, for descriptive purposes, into sections that correspond to the chemical reactions given in the equations and shown on Fig. 1.

Both the 1979 and 1981 flowsheets used phosphoric acid to extract the water from the HI_x ($\text{HI}/\text{I}_2/\text{H}_2\text{O}$) solution resulting from the Bunsen reaction. No hydrogen cost estimates were made using the 1979 flowsheet but the cost estimates for the 1981 flowsheet indicated that over 40% of the total capital cost of the process was associated with the phosphoric acid extraction step.

There were a number of suggestions as to methods of modifying the process to reduce the capital cost. Subsequently, measurements of vapor-liquid equilibria for the system $\text{HI}/\text{I}_2/\text{H}_2\text{O}$ were made in Germany and German researchers (Roth and Knoche) produced a partial flowsheet that indicated that reactive distillation could work. [6]. We evaluated the possible

flowsheet variations and decided to pursue the reactive distillation scenario as the primary effort but to maintain the H_3PO_4 variation as a backup.

The overall process naturally divides itself into process sections in which there is significant recycle and interconnection and which are connected to the other sections by a minimum number of streams. For the Sulfur-Iodine cycle, these natural sections roughly correspond to the chemical reactions. The flowsheet associated with each chemical reaction and its attendant separation processes is numbered. Section 1, 2 and 3 are used to designate the portions of the flowsheet associated with the Bunsen reaction (where the acids are formed,) the sulfuric acid decomposition reaction and the hydrogen iodide decomposition reaction.

Chemical flowsheet simulator – The early flowsheets for the S-I cycle were all developed based on hand calculations. Attempts were made to use chemical flowsheet simulation programs but the programs available at that time were unable to handle extremely non-ideal systems such as those found in the sulfur-iodine thermochemical water-splitting cycle. Significant advances have been made in understanding the thermodynamics of aqueous ionic systems since the time of the earlier flowsheeting efforts. It was our intent to develop thermodynamic models compatible with a modern chemical flowsheet simulator and perform extensive process optimization studies to best match the reactor to the thermochemical process.

The chemical process simulator we found best for handling our non-ideal chemical systems is Aspen Plus®, Aspen Technology, Inc. (AspenTech.) [7]. Aspen Plus® incorporates the capability of modeling electrolytes via several different modeling techniques including an electrolytic version of the non-random two liquid (NRTL) technique. An electrolytic NRTL model (ELECNRTL) model can handle everything from concentrated electrolytes through dilute electrolytes to non-polar species, such as iodine, so it should be able to handle the chemistry of the sulfur-iodine cycle. In fact, Aspen Plus® included an ELECNRTL model for sulfuric acid, good to 200°C, right out of the box. In addition, Aspen Plus® includes the capability of simultaneously regressing model parameters of many different types in order to generate a thermodynamic model for a specific chemical system. Aspen Plus® was chosen as the process simulator for this work.

Development of thermodynamic models – An NRTL model describes a chemical system in terms of the thermodynamic parameters for the pure components along with pair-wise parameters, which describe the interactions between each pair of pure components. The electrolytic variation (ELECNRTL) adds a description of the ionic associations and dissociations along with pure component and pair-wise parameters for the ionic species with each other and with the nonionic species present. Our plan of attack was to use the existing ELECNRTL model for sulfuric acid, describing the system H_2SO_4/H_2O , and use this model for developing the flowsheet for Section 2. Simultaneously, we would develop a new ELECNRTL model for the system $HI/I_2/H_2O$, which used the same pure component properties for water as used in the sulfuric acid model, and use this model to develop the flowsheet for Section 3. Finally we would develop a model for the system $H_2SO_4/HI/I_2/H_2O$, using the pure component and pair-wise components of the earlier models along with pair-wise parameters that were undefined in the simpler models, for the Section 1 flowsheeting effort. The first two models would need to be valid over wide ranges of temperature and pressure, as operating conditions for Sections 2 and 3 may need to be varied widely in order to optimize the overall flowsheet but the final model would only need to be valid over the limited range of temperatures and pressures for which sulfuric acid and hydrogen iodide form separate condensed phases.

Although sulfuric acid is one of the most common industrial chemicals, it is almost never concentrated by thermal means. (Concentrated sulfuric acid is produced commercially at low temperatures by adsorbing SO_3 in dilute sulfuric acid.) Previous work had shown that optimal configurations for Section 2 involved performing some of the concentration steps at high pressure (and temperature) so that the condensing temperature of the distillate was high enough to reuse the heat elsewhere in the process. The maximum temperature of the existing liquid sulfuric acid model was 200°C and we would require a model that was valid at temperatures on the order of 300°C.

Experts at Aspen Technologies have developed techniques which allow them to regress difficult systems. We elected to subcontract the regression task to Aspen Technologies. The resulting ELECNRTL sulfuric acid model is a very good representation of the system and was used in our Section 2 flowsheet.

The $\text{HI}/\text{I}_2/\text{H}_2\text{O}$ regression was not as successful. The final model accurately describes the "iodine lean" liquid-liquid equilibrium (LLE) region but its description of the "hydrogen iodide lean" LLE region is suspect. There are no data for this region, except for the hydrogen iodide free endpoints, but the shape of this LLE boundary is irregular. More telling is the fact that Aspen Plus® was unable to converge multistage vapor-liquid equilibrium (VLE) processes that are the basis for the reactive distillation flowsheet for Section 3.

We were unable to tell, with the aid of Aspen Technologies, whether the model was too complicated for Aspen Plus® or if there were physically unrealizable conditions predicted by the model. That the model might predict physically unrealizable conditions is not surprising as no vapor composition data were used in the regression that generated the model. In fact the only VLE data available are total pressure data and these data are further confounded by the fact that the pressure measurement includes the equilibrium decomposition of hydrogen iodide into hydrogen and iodine. The model is able to converge for a single stage VLE process therefore it is useful for predicting physical properties a given state but not the rate of change of properties with change in state. Likewise, the overall model for $\text{H}_2\text{SO}_4/\text{HI}/\text{I}_2/\text{H}_2\text{O}$ could be used to predict physical properties, but was unable to predict chemical equilibrium due to the sparsity of thermal data for the system. These two models were used extensively in the equipment sizing calculations, which were the basis of the economic analysis, but were not used in generating the final flowsheets.

FLOWSCHEETS

The flowsheets for the three sections are shown here. The streams are labeled the figures and the temperature, pressure, and molar flowrate for each stream are given in the tables. The flowrates are normalized to the production of one mole of hydrogen in the overall plant.

Bunsen Reaction (Section 1) – As Roth and Knoche based their flowsheet on the 1979 flowsheet we needed to use a Section 1 flowsheet that produced the same feed stream to Section 3 and also had the high recycle of hydrogen iodide necessary for the reactive distillation flowsheet. The flowsheet is shown in Fig. 2 and Table 1.

Sulfuric Acid Concentration and Decomposition (Section 2) – The sulfuric acid portion of the process is, to a large part, decoupled from the rest of the process. Once the ratio of sulfuric acid to water was defined, Section 2 could be optimized separately. The final flowsheet for Section 2, generated using Aspen Plus®, is shown in Fig. 3 and Table 2. Section 2 is normalized for the decomposition of one mole of sulfuric acid and the production of one mole each of oxygen and sulfur dioxide. Before the sulfuric acid can be decomposed it must first be concentrated. The concentrated acid is vaporized and decomposed. The undecomposed sulfuric acid is recycled within Section 2 to the extent practical. The overall flow scheme is based on the 1981 flowsheet [5].

Hydrogen Iodide Decomposition (Section 3) – The reactive distillation flowsheet was based on information presented by Roth and Knoche [6]. As indicated previously, multi-staged VLE equipment could not be converged with our $\text{HI}/\text{I}_2/\text{H}_2\text{O}$ model. In the end we were forced to abandon our attempts at optimizing the reactive distillation flowsheet and instead use the flowsheet presented by Roth and Knoche. This flowsheet has a large recycle of undecomposed HI from Section 3 back to Section 1. Only about 16% of the HI is decomposed in a single pass. This recycle, together with the approximately factor of five excess iodine required in the product flow stream from Section 1 to Section 3 and the equal amount of water, means that for each mole of hydrogen produced, approximately 6 moles of HI, 30 moles of iodine and 30 moles of water must flow from Section 1 to Section 3, and 5 moles of HI, 30 moles of iodine and 30 moles of water must flow back from Section 3 to Section 1.

The reactive distillation Section 3 flowsheet is present in Fig. 4 and Table 3.

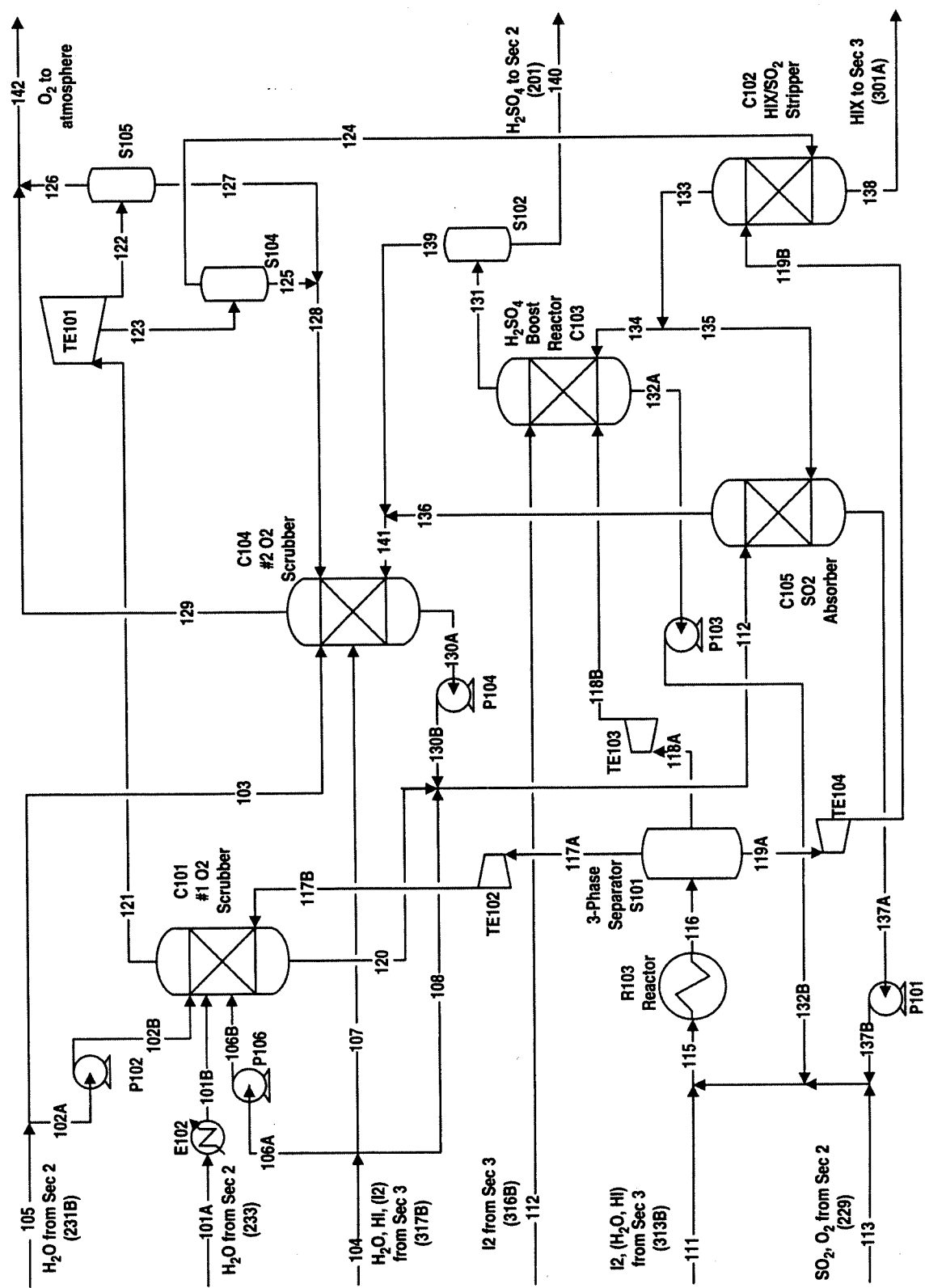


Figure 2. Section 1 flowsheet.

Table 1. Material Balance Section 1 — Main Solution Reaction

Stream	H ₂ SO ₄	HI	I ₂	H ₂ O	SO ₂	O ₂	Total	Phase	P Bar	T K
101A	0.0222	0.0000	0.0000	3.4582	0.0078	0.0000	3.4882	L	4.2	393.15
101B	0.0222	0.0000	0.0000	3.4582	0.0078	0.0000	3.4882	L	4.2	359.6
102A	0.0002	0.0000	0.0000	0.3186	0.0000	0.0000	0.3188	L	1.01	311.15
102B	0.0002	0.0000	0.0000	0.3186	0.0000	0.0000	0.3188	L	4.4	311.15
103	0.0010	0.0000	0.0000	1.2847	0.0000	0.0000	1.2857	L	1.01	311.15
104	0.0000	9.5997	5.6840	62.4940	0.0000	0.0000	77.7777	L	4.2	368.51
105	0.0012	0.0000	0.0000	1.6033	0.0000	0.0000	1.6045	L	1.01	311.15
106	0.0000	0.2880	0.1705	1.8742	0.0000	0.0000	2.3327	L	1.85	311.15
107	0.0000	0.0806	0.0477	0.5248	0.0000	0.0000	0.6531	L	1.01	368.51
108	0.0000	9.2311	5.4658	60.0950	0.0000	0.0000	74.7919	L	4.2	368.51
110	0.0000	0.0011	0.8810	0.0170	0.0000	0.0000	0.8991	L	1.85	393
111	0.0000	0.8582	42.4423	4.2056	0.0000	0.0000	47.5061	L	1.85	393
112	0.2173	9.9875	5.5163	67.2589	0.0000	0.0000	82.9800	L	1.85	-
113	0.0000	0.0000	0.0000	0.0328	0.9961	0.5000	1.5289	V	7	393
115	0.2173	10.9846	48.7791	72.7279	2.2660	0.5000	135.4749	V+L	7	-
116	0.9545	12.4590	48.0419	71.2535	1.5288	0.5000	134.7377	V+L	7	393
117A	0.0000	0.0000	0.0075	0.0338	0.1424	0.5000	0.6837	V	7	393
117B	0.0000	0.0000	0.0075	0.0338	0.1424	0.5000	0.6837	V	4.2	354.2
118A	0.9545	0.0000	0.0000	5.1520	0.0154	0.0000	6.1219	L	7	393
118B	0.9545	0.0000	0.0000	5.1520	0.0154	0.0000	6.1219	L	1.85	393
119A	0.0000	12.4590	48.0344	66.0677	1.3710	0.0000	127.9321	L	7	393
119B	0.0000	12.4590	48.0344	66.0677	1.3710	0.0000	127.9321	L	1.85	393
120	0.1726	0.5884	0.0278	5.3694	0.0000	0.0000	6.1582	L	4.2	384.4
121	0.0000	0.0000	0.0000	0.0150	0.0000	0.5000	0.5150	V	4.2	384.4
122	0.0000	0.0000	0.0000	0.0095	0.0000	0.3175	0.3270	L+V	1.01	-
123	0.0000	0.0000	0.0000	0.0055	0.0000	0.1825	0.1880	L+V	1.85	289
124	0.0000	0.0000	0.0000	0.0027	0.0000	0.1825	0.1852	V	1.85	289
125	0.0000	0.0000	0.0000	0.0028	0.0000	0.0000	0.0028	L	1.85	289
126	0.0000	0.0000	0.0000	0.0051	0.0000	0.3175	0.3226	V	1.01	-
127	0.0000	0.0000	0.0000	0.0044	0.0000	0.0000	0.0044	L	1.01	-
128	0.0000	0.0000	0.0000	0.0072	0.0000	0.0000	0.0072	L	1.01	-
129	0.0000	0.0000	0.0000	0.0142	0.0000	0.1825	0.1967	V	1.01	313
130A	0.0447	0.1680	0.0227	1.7945	0.0000	0.0000	2.0299	L	1.01	393
130B	0.0447	0.1680	0.0227	1.7945	0.0000	0.0000	2.0299	L	1.85	393
131	1.0234	0.0000	0.0184	4.1377	0.0475	0.0155	5.2425	L	1.85	384.5
132A	0.0000	0.1389	0.7960	0.9252	0.0155	0.0000	1.8756	L	1.85	384.5
132B	0.0000	0.1389	0.7960	0.9252	0.0155	0.0000	1.8756	L	7	384.5
133	0.0000	0.0000	0.0271	0.3731	1.3710	0.1825	1.9537	V	1.85	393
134	0.0000	0.0000	0.0023	0.0317	0.1165	0.0155	0.1660	V	1.85	393
135	0.0000	0.0000	0.0248	0.3414	1.2545	0.1670	1.7877	V	1.85	393
136	0.0000	0.0000	0.0003	0.0360	0.0001	0.1670	0.2034	V	1.85	369.6
137A	0.2173	9.9875	5.5408	67.5643	1.2544	0.0000	84.5643	L	1.85	369.6
137B	0.2173	9.9875	5.5408	67.5643	1.2544	0.0000	84.5643	L	7	369.6
138	0.0000	12.4590	48.0073	65.6973	0.0000	0.0000	126.1636	L	1.85	393
139	0.0000	0.0000	0.0184	0.0434	0.0436	0.0155	0.1209	V	1.85	384.5
140	1.0234	0.0000	0.0000	4.0943	0.0039	0.0000	5.1216	L	1.85	384.5
141	0.0000	0.0000	0.0187	0.0794	0.0437	0.1825	0.3243	V	1.85	375.15
142	0.0000	0.0000	0.0000	0.0193	0.0000	0.5000	0.5193	V	1.01	-

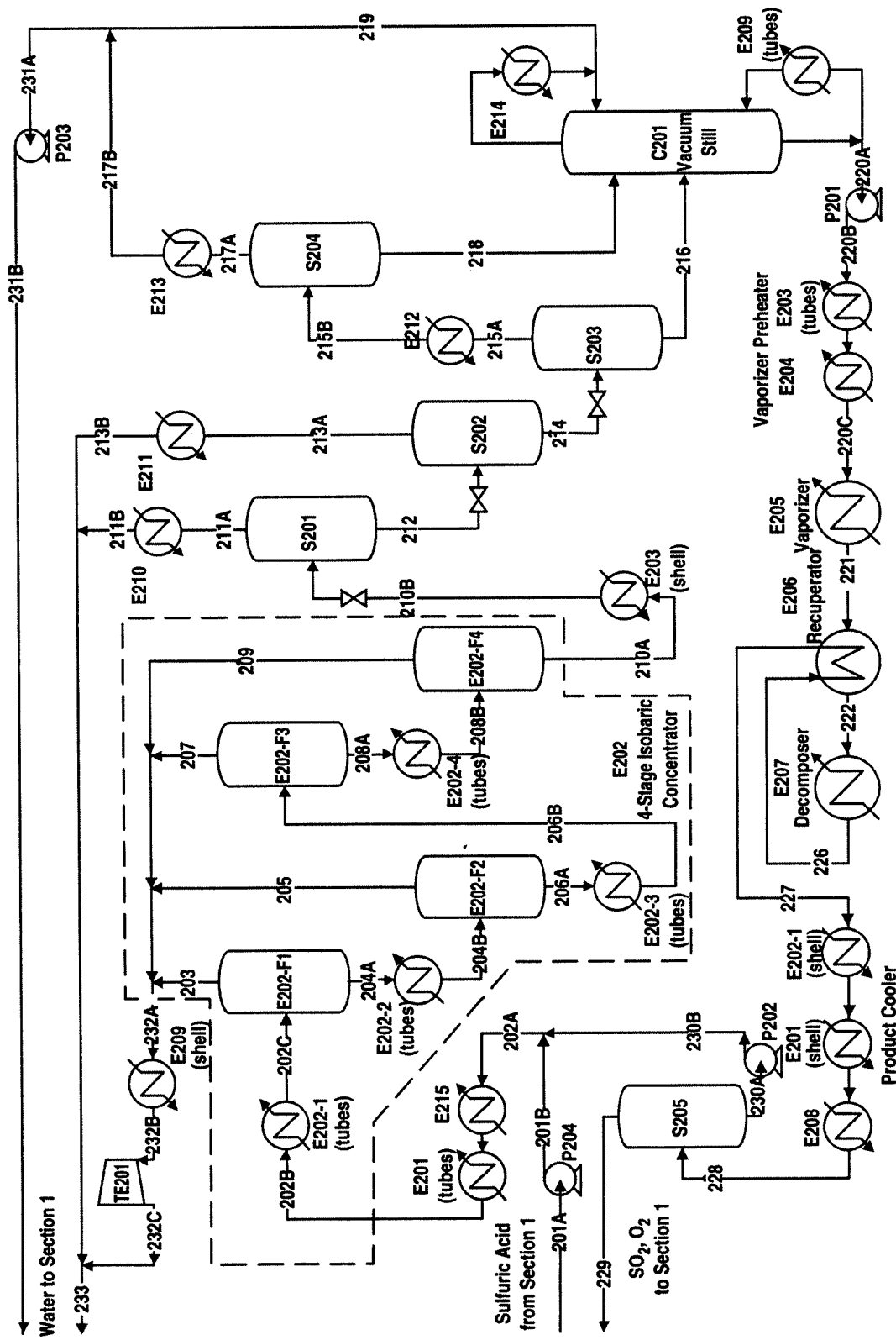


Figure 3. Section 2 flowsheet.

Table 2. Material Balance for Section 2, Sulfuric Acid Decomposition

Stream	H ₂ O	H ₂ SO ₄	SO ₃	O ₂	SO ₂	Total	Phase	Press. Bar	Temp K
201	4.0943	1.0234	0	0	0.0039	5.1216	L	35	393.15
202A	5.2361	1.6298	0	0	0.0078	6.8737	L	35	572.15
202B	5.2361	1.6298	0	0	0.0078	6.8737	L + V	35	603.15
203	1.0007	0.0018	0	0	0.0052	1.0077	V	35	603.15
204A	4.2354	1.628	0	0	0.0026	5.866	L	35	603.15
204B	4.2354	1.628	0	0	0.0026	5.866	L + V	35	619.15
205	0.8661	0.0038	0	0	0.0019	0.8718	V	35	619.15
206A	3.3693	1.6242	0	0	0.0007	4.9942	V	35	619.15
206B	3.3693	1.6242	0	0	0.0007	4.9942	L + V	35	631.15
207	0.5037	0.0039	0	0	0.0004	0.508	V	35	631.15
208A	2.8656	1.6203	0	0	0.0003	4.4862	L	35	631.15
208B	2.8656	1.6203	0	0	0.0003	4.4862	L + V	35	644.15
209	0.433	0.0056	0	0	0.0002	0.4388	V	35	644.15
210A	2.4326	1.6147	0	0	0.0001	4.0474	L	35	644.15
210B	2.4326	1.6147	0	0	0.0001	4.0474	L	35	581.15
211A	0.273	0.002	0	0	0.0001	0.2751	V	8	562.85
211B	0.273	0.002	0	0	0.0001	0.2751	L	8	393.15
212	2.1596	1.6127	0	0	0	3.7723	L	8	562.85
213A	0.3817	0.0051	0	0	0	0.3868	V	2	517.05
213B	0.3817	0.0051	0	0	0	0.3868	L	2	393.15
214	1.7779	1.6076	0	0	0	3.3855	L	2	517.05
215A	0.5471	0.0134	0	0	0	0.5605	V	0.07	432.85
215B	0.5471	0.0134	0	0	0	0.5605	V + L	0.07	408.15
216	1.2308	1.5942	0	0	0	2.825	L	0.07	432.85
217A	0.5335	0.0012	0	0	0	0.5347	V	0.07	408.15
217B	0.5335	0.0012	0	0	0	0.5347	L	0.07	311.15
218	0.0136	0.0122	0	0	0	0.0258	L	0.07	408.15
219	1.0698	0	0	0	0	1.0698	L	0.07	311.15
220A	0.1746	1.6064	0	0	0	1.781	L	0.07	485.25
220B	0.1746	1.6064	0	0	0	1.781	L	7	486.05
220C	0.1746	1.6064	0	0	0	1.781	L	7	684.15
221	0.6174	1.1636	0.4428	0	0	2.2238	L + V	7	684.15
222	1.4899	0.2911	1.3153	0	0	3.0963	V	7	796.85
223	1.7	0.081	1.261	0.1322	0.2644	3.4386	V	7	875.05
224	1.757	0.024	1.0776	0.2524	0.5048	3.6158	V	7	955.05
225	1.7725	0.0085	0.8405	0.3787	0.7574	3.7576	V	7	1027.05
226	1.7777	0.0033	0.6031	0.5	1	3.8841	V	7	1100.15
227	1.4456	0.3354	0.271	0.5	1	3.552	V	7	704.15
228	1.1746	0.6064	0	0.5	1	3.281	L + V	7	393.15
229	0.0328	0	0	0.5	0.9961	1.5289	V	7	393.15
230A	1.1418	0.6064	0	0	0.0039	1.7521	L	7	393.15
230B	1.1418	0.6064	0	0	0.0039	1.7521	L	35	396.05
231A	1.6033	0.0012	0	0	0	1.6045	L	0.07	311.15
231B	1.6033	0.0012	0	0	0	1.6045	L	1.01	311.25
232A	2.8035	0.0151	0	0	0.0077	2.8263	V	35	621.35
232B	2.788	0	0	0	0.0038	2.7918	L	35	393.15
232C	2.788	0	0	0	0.0038	2.7918	L	5.2	393.15
233	3.4582	0.0222	0	0	0.0078	5.2058	L	5.2	393.15

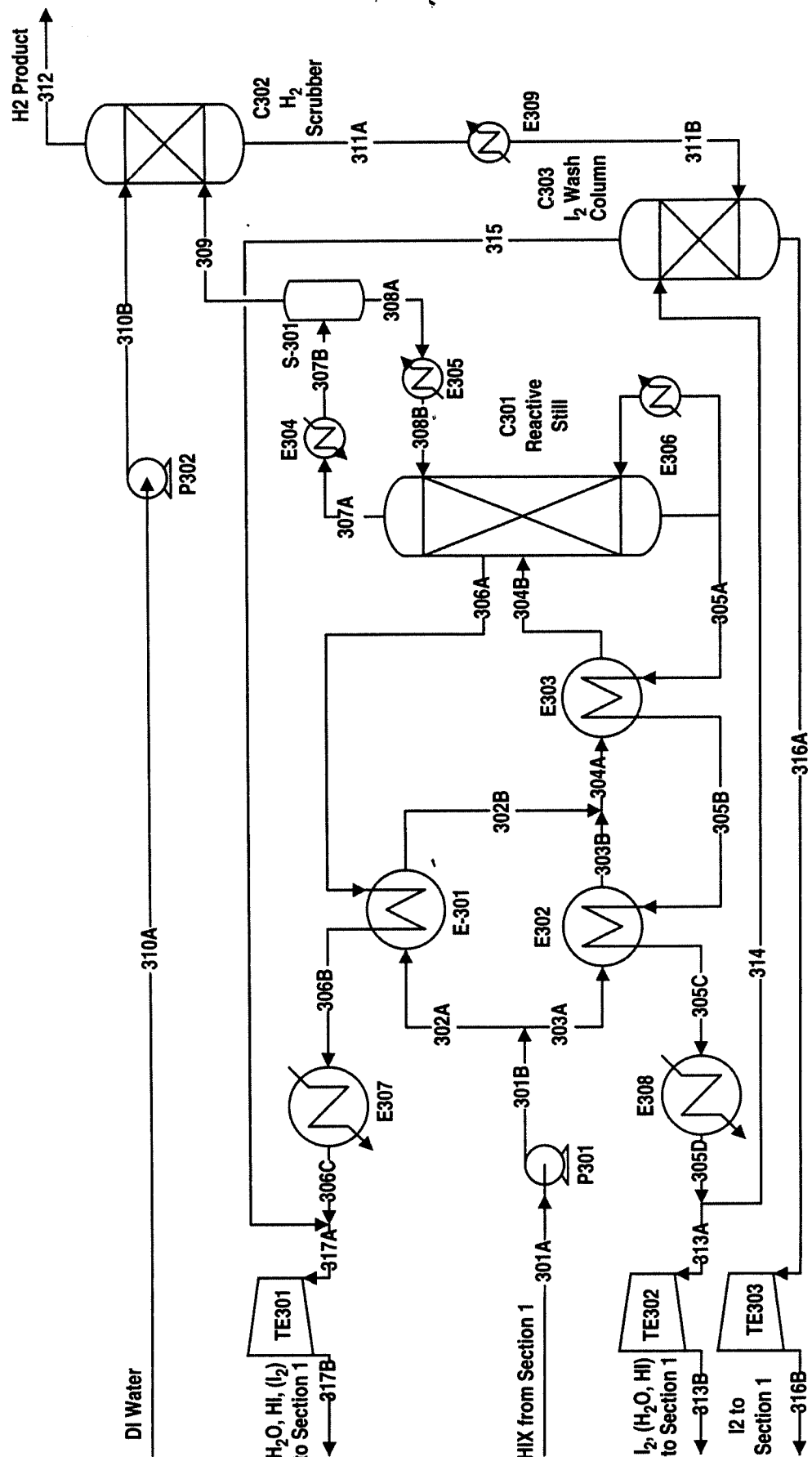


Figure 4. Section 3 flowsheet.

Table 3. Material Balance for Section 3 HI Decomposition								
Stream ID	HI	I ₂	H ₂ O	H ₂	Total	Phase	Press. Bar	Temp K
301A	12.4590	48.0073	65.6973	0.0000	126.1636	L	1.85	393.15
301B	12.4590	48.0073	65.6973	0.0000	126.1636	L	22	393.15
302A	7.7869	30.0046	41.0608	0.0000	78.8523	L	22	393.15
302B	7.7869	30.0046	41.0608	0.0000	78.8523	L	22	511.04
303A	4.6721	18.0027	24.6365	0.0000	47.3113	L	22	393.15
303B	4.6721	18.0027	24.6365	0.0000	47.3113	L	22	511.04
304A	12.4590	48.0073	65.6973	0.0000	126.1636	L	22	511.04
304B	12.4590	48.0073	65.6973	0.0000	126.1636	L	22	535.15
305A	0.8763	43.3367	4.2941	0.0000	48.5071	L	22	583.15
305B	0.8763	43.3367	4.2941	0.0000	48.5071	L	22	521.44
305C	0.8763	43.3367	4.2941	0.0000	48.5071	L	22	401.05
305D	0.8763	43.3367	4.2941	0.0000	48.5071	L	22	393.15
306A	9.5787	5.6706	61.3805	0.0000	76.6298	L	22	524.15
306B	9.5787	5.6706	61.3805	0.0000	76.6298	L	22	403.15
306C	9.5787	5.6706	61.3805	0.0000	76.6298	L	22	368.15
307A	0.5333	0.0000	1.8000	1.0000	3.3333	V	22	494.15
307B	0.5333	0.0000	1.8000	1.0000	3.3333	V+L	22	298.15
308A	0.5293	0.0000	1.7773	0.0000	2.3066	L	22	298.15
308B	0.5293	0.0000	1.7773	0.0000	2.3066	L	22	494.15
309	0.0040	0.0000	0.0227	1.0000	1.0267	V	22	298.15
310A	0.0000	0.0000	1.0207	0.0000	1.0207	L	1.013	298.15
310B	0.0000	0.0000	1.0207	0.0000	1.0207	L	22	298.15
311A	0.0040	0.0000	1.0420	0.0000	1.0460	L	22	298.15
311B	0.0040	0.0000	1.0420	0.0000	1.0460	L	22	393.15
312	0.0000	0.0000	0.0014	1.0000	1.0014	V	22	298.15
313A	0.8582	42.4423	4.2056	0.0000	47.5061	L	22	393.15
313B	0.8582	42.4423	4.2056	0.0000	47.5061	L	7	393.15
314	0.0181	0.8944	0.0885	0.0000	1.0010	L	22	393.15
315	0.0210	0.0134	1.1135	0.0000	1.1479	L	22	393.15
316A	0.0011	0.8810	0.0170	0.0000	0.8991	L	22	393.15
316B	0.0011	0.8810	0.0170	0.0000	0.8991	L	7	393.15
317A	9.5997	5.6840	62.4940	0.0000	77.7777	L	22	368.51
317B	9.5997	5.6840	62.4940	0.0000	77.7777	L	4.2	368.51

SIZING AND COST ESTIMATES

Reactor Matching – We wished to evaluate the economic potential for hydrogen produced from nuclear energy in a mature hydrogen economy. The scenario chosen was that of a large hydrogen plant located on a major hydrogen pipeline. The standard gas cooled reactor complex is a cluster of four 600 MW(t) GT-MHR's [8]. Cost estimates for the GT-MHR are available and served as the basis of our estimate of an H₂-MHR. The four-reactor cluster makes sense from an availability basis because fueling can be staggered and the plant can be kept at a minimum of 75% capacity at all times.

The nuclear reactor must be matched to the chemical process such that high thermal efficiency is obtained, but not at the expense of sacrificing the operability of the combined plant. We chose to restrict thermal energy recovery to recovery within a section and to exclude recovery between sections in order to minimize the effect of flow or composition transients in one section on the operational stability of other sections. Section 1 requires no thermal energy, it is an exporter of heat to the environment. Temperatures are much higher in Section 2 than Section 3 and the theoretical energy requirements of Section 2 are much larger than Section 3, therefore the major effect of this decision is to rule out transfer of waste heat from Section 2 to Section 3. This decision resulted in a lower thermal efficiency than could have otherwise been achieved,

perhaps needlessly, as the thermal coupling between sections is inherently very high, despite the lack of direct flows between them, because both Sections 2 and 3 are strongly coupled via flows to and from Section 1.

Sandia National Laboratory considered two approaches to coupling the reactor to the chemical plant. For the simpler approach, high temperature helium from the reactor is split into two streams, which power Sections 2 and 3 in parallel. For our design point, shown in the figures and tables above, this approach led to an efficiency of 42%. In the second approach, the helium flow is similar but, instead of heating Section 3 directly, Section 3 is heated by the waste heat from a Brayton cycle. This approach led to a total efficiency (hydrogen plus electricity) of 48% when half the output is hydrogen. This is an indication that further optimization of the S-I process, with coupling of energy between Sections 2 and 3, may lead to higher efficiency for hydrogen production even at the design point of 827°C peak process temperature.

Using the design point flowsheet, we estimated the higher efficiency that could be achieved by raising the peak process temperature. The results, shown on Fig. 5, indicate that we could achieve an hydrogen production efficiency of 51% at 900°C peak process temperature.

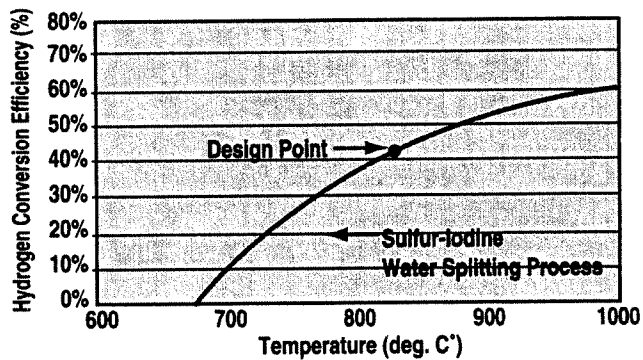


Figure 5. Estimated S-I Process Hydrogen Production Efficiency vs. Peak Process Temperature.

Component Sizing – Standard chemical engineering methods were used to size the chemical process equipment. The diameters of packed and tray columns were determined utilizing the Leva generalized pressure drop correlation (GPDC) as presented by Seader [9]. The minimum interfacial area for process vessels was determined such that vapor velocities were insufficient to entrain macroscopic liquid droplets. For vertical vessels the minimum diameter is calculated directly from the minimum interfacial area and the height is determined on the basis of residence time. For horizontal vessels, the minimum diameter is calculated by adjusting the L/D ratio to obtain the desired residence time. The residence time for each vessel was determined on a case-by-case basis via engineering judgment.

The method used for sizing heat exchangers is presented in Perry's Chemical Engineers' Handbook [10]. All fluid properties used in the sizing calculations were determined using Aspen Plus 10.2 software [7], the same software used in the flowsheet modeling. In addition, all power requirement for pumps, compressors, and turbines were all sized using Aspen Plus.

Component Costing – Capital cost estimates were generated using the Guthrie method as modified by Ulrich [11]. Generally the cost per unit of capacity or size decreases with size until some maximum size is reached. If the maximum size or capacity is reached, multiple parallel units are called required. Most of the chemical plant equipment is at the maximum size suggested by the costing algorithms. Under these conditions the majority of the economies of scale have been taken. The resulting total capital costs are shown in Table 4. All costs are in 2002 dollars.

Table 4. Preliminary capital cost estimate — Summary — 4200 mole/s — Year 2002 \$

Description	Hardware Cost (\$K)	Bare Module Cost (\$K)	Bare Module Cost Plus Adders (\$K)
Subtotals for Section 1	7,720	42,492	72,706
Subtotals for Section 2	9,319	122,133	144,063
Subtotals for Section 3	23,737	155,350	275,021
Total Hardware Cost	40,776		
Total Bare Module Cost		319,975	
Total Bare Module Cost with adders (liners, insulation, etc.)			491,790
Contingency and Fee			88,522
Total Module Cost			594,584
Auxiliary Facilities Cost			14,272
Total Capital Cost			594,584
Initial Chemical Inventory			114,802
Total Capital Investment			709,386

Flowsheet Cost Comparison — The flowsheets presented above produces 4200 moles/s of hydrogen at 42% efficiency. The thermal power required to drive this thermochemical process is 2,857 MW(t). The normalized capital cost per unit thermal energy, then, is \$595 M divided by 2,857 MW(t), or \$208/kW(t). As the process efficiency is raised, either by higher peak process temperature or by further process optimization, the amount of thermal energy that must be handled to produce a given amount of hydrogen will decrease. The scale of the chemical plant is such that there are usually five or more parallel equipment trains. Therefore we believe the normalized capital cost per unit thermal energy will be relatively unchanged and we will use the \$208/kW(t) number in our analysis below. The S-I plant also has a large inventory of iodine, estimated at 8,830 tonnes. At \$13,000/t, this will add \$40/kW(t) to the normalized capital cost.

The 1981 flowsheet [5] based on the use of phosphoric acid to remove water from Section 3 had a normalized capital cost of \$315/kW(t). It achieved 38% hydrogen production efficiency with a peak process temperature of 827°C. The 1979 flowsheet had 47% efficiency at 871°C but was not costed. The flowsheet presented here has 42% efficiency at 827°C and is projected to achieve a 51% efficiency at 900°C and to have a normalized capital cost of \$208/kW(t). The reactive distillation process for HI decomposition appears to be able to achieve the promise that Roth and Knoche predicted [6]. We have adopted it for our continuing development of the Sulfur-Iodine thermochemical water-splitting cycle.

Estimated Cost of Hydrogen — With cost and efficiency estimates for the S-I cycle in hand, it is useful to estimate the cost of hydrogen produced by this process. The projected cost of an "Nth of a kind" Gas Turbine-Modular Helium reactor is \$975/kW(e) [8]. This is for a 2,400 MW(t), four module plant that would be consistent with the assumptions made in costing the S-I process plant. The normalized cost per unit thermal energy is \$465/kW(t). By subtracting the cost of the turbogenerator systems and adding the cost of helium circulators and heat exchangers, we estimate the cost of a process heat version of the Modular Helium Reactor as \$326/kW(t). The GT-MHR operates with an outlet temperature of 850°C. Since we wish to operate the S-I process at 900°C, we made rough estimates of cost increases that might be needed to operate the MHR at 950°C outlet temperature. This raises the normalized cost to \$371/kW(t). We also need an intermediate heat transport loop to carry the heat from the reactor to the S-I process. This is estimated to cost \$43/kW(t). So the total cost of the heat supply system for the hydrogen plant is \$371 + \$43 = \$414/kW(t). The hydrogen production plant costs \$208/kW(t). The chemical inventory adds \$40/kW(t). The total unit capital cost is \$414 + \$208 + \$40 = \$662/kW(t). Adding interest during construction raises this to \$715/kW(t).

The annual capital recovery charge, using the normal rate structure for a regulated utility is 12.6% of total capital. Assuming 90% availability, the capital recovery charges are $\$715 \times 0.126/(8760 \times 0.9) = \$11.4/\text{MW(t-h)}$. The fuel cycle and operations and maintenance costs of the reactor are $\$4.6/\text{MW(t-h)}$. The operations and maintenance cost of the S-I plant is estimated at 7% of initial capital/year or $\$2.3/\text{MW(t-h)}$. The total cost of hydrogen is $\$11.4 + 4.6 + 2.3 = \$18.3/\text{kW(t-h)}$.

At 51% efficiency, 1 kW(t-h) will produce 12.9 kg of hydrogen. Thus the estimated cost of hydrogen from a large-scale, Nth of a kind plant will be $\$18.3/12.9 = \1.42 per kg of hydrogen. This corresponds roughly to cost estimates of hydrogen produced by steam reformation of methane when the cost of natural gas reaches $\$6.20/\text{MBtu}$.

SUMMARY

We have developed the flowsheet for a large-scale hydrogen production plant based on the Sulfur-Iodine thermochemical water-splitting cycle, driven by high temperature heat from a modular helium reactor. The flowsheet is based on use of reactive distillation to decompose the hydrogen iodide. We compared our results with earlier flowsheets that used a phosphoric acid process to extract water from the HI-H₂O mixture, followed by thermal decomposition of the HI. The flowsheet presented here promises somewhat higher efficiency and reduced capital cost compared to the earlier flowsheets. Cost estimates for the production of hydrogen from a plant based on this flowsheet project reasonable costs for hydrogen.

The flowsheet analysis is extremely challenging, particularly for Section 3, HI Decomposition. We have had to make a number of assumptions to complete our analysis. Additional chemical thermodynamic data are needed for the HI-I₂-H₂O system, and improved calculational models need to be developed that are consistent with these data. The attractive results we have obtained give impetus to carry out the R&D needed to improve the data and models.

The flowsheets presented here were not strongly coupled thermally between Section 2, H₂SO₄ Decomposition and Section 3, HI Decomposition. It may be possible to get further flowsheet improvements by using heat from Section 2 to drive the reactions in Section 3. This could allow reduction in the 900°C peak process temperature needed to achieve 50% efficiency, or could allow still higher efficiency to be obtained at this temperature. These opportunities need to be explored when improved data and models have been developed.

ACKNOWLEDGMENTS

Prepared under the Nuclear Energy Research Initiative (NERI) Program from the US Department of Energy under Grant No. DE-FG03-99SF21888.

REFERENCES

1. L. C. Brown, J. F. Funk, P. Pickard, A. Marshall and S. K. Showalter, "High Efficiency Generation of Hydrogen Fuels Using Nuclear Power - Final Report," General Atomics report to be issued, 2003.
2. L. C. Brown, et al., "High Efficiency Generation Of Hydrogen Fuels Using Thermochemical Cycles And Nuclear Power," AIChE 2002 Spring Meeting, March 11-15, 2002.
3. A. C. Marshall, "An Assessment of Reactor Types for Thermochemical Hydrogen Production," Sandia National Laboratories Report to DOE, August 2001.
4. J. H. Norman, G. E. Besenbruch, D. R. O'Keefe and C. L. Allen, "Thermochemical Water-Splitting Cycle, Bench-Scale Investigations, and Process Engineering, Final Report for the Period February 1977 through December 31, 1981," General Atomics Report GA-A16713, DOE Report DOE/ET/26225-1.
5. R. H. Werner, ed. "Synfuels from Fusion — Using the Tandem Mirror Reactor and a Thermochemical Cycle to Produce Hydrogen," Lawrence Livermore Laboratory Report UCID-19609, November 1, 1982.
6. M. Roth and K. F. Knoche, "Thermochemical Water-Splitting Through Direct HI-Decomposition from H₂O/HI/I₂ Solutions," Int. J. Hydrogen Energy 14, 545-549, 1989.
7. Aspen Plus, Version 10.2, Aspen Technology, Inc., 2000.
8. M. P. LaBar, "The Gas-Turbine-Modular Helium Reactor: A Promising Option for Near-Term Deployment," Intl. Cong. on Advanced Nuclear Power Plants, June 2002, Hollywood, Florida.

9. J. D. Seader, E. J. Henley, *Separation Process Principles*, Wiley, New York, 1998.
10. D. W. Green, Ed., *Perry's Chemical Engineers' Handbook*, Seventh Ed., McGraw Hill, New York, 1997.
11. G. D. Ulrich, *A Guide to Chemical Engineering Process Design and Economics*, Wiley, New York, 1984.

CONTACT

Lloyd C. Brown
General Atomics
P.O. Box 85608
San Diego, CA,
92186-5608 USA
Phone: 858-455-3078
e-mail: lloyd.brown@gat.com

